Giant optomechanical coupling and dephasing protection with cavity exciton-polaritons

P. Sesin [1,2] A. S. Kuznetsov,[3] G. Rozas [1,2] S. Anguiano [1,2] A. E. Bruchhausen,[1,2] A. Lemaître,[4]
K. Biermann [3] P. V. Santos,[3,*] and A. Fainstein [1,2,†]

[1]*Centro Atómico Bariloche and Instituto Balseiro, Comisión Nacional de Energía Atómica (CNEA) - Universidad
Nacional de Cuyo (UNCUYO), 8400 Bariloche, Argentina*
[2]*Instituto de Nanociencia y Nanotecnología (INN-Bariloche), Consejo Nacional de Investigaciones
Científicas y Técnicas (CONICET), Argentina*
[3]*Paul-Drude-Institut für Festkörperelektronik, Leibniz-Institut im Forschungsverbund Berlin e.V., Hausvogteiplatz 5-7, 10117 Berlin, Germany*
[4]*Université Paris-Saclay, CNRS, Centre de Nanosciences et de Nanotechnologies, 91120 Palaiseau, France*

Electronic resonances can significantly enhance photon-phonon coupling but are normally avoided in cavity optomechanics due to absorption losses and dephasing by inhomogeneous broadening. We demonstrate experimentally that exciton-polaritons in semiconductor microcavities enable single-particle resonant optomechanical couplings with GHz vibrations reaching record values in the tens of MHz range. Moreover, this resonant enhancement is protected from inhomogeneous broadening by the Rabi gap. Single-polariton nonlinearities and the optomechanical strong-coupling regime become accessible in this platform.

The search for strong optical forces (i.e., large optomechanical coupling factor g_0) is relevant to attain optomechanical (OM) cooling and self-oscillation [1] and to access the OM strong-coupling regime [1–4]. Single-photon OM nonlinearities are accessible when the cooperativity $C_0 = 4g_0^2/\kappa\Gamma > 1$, with κ and Γ being the optical and mechanical dissipation rates, respectively [1]. For the multiple-photon case, the OM coupling is amplified as $g_{\text{eff}} = g_0\sqrt{N_p}$ [1], with N_p being the photon number. The OM strong-coupling regime $g_{\text{eff}} > \kappa, \Gamma$ [1] thus requires large g_0 and small κ and Γ, but can also be enforced by strong pumping. Typically, cavity-OM systems rely on radiation-pressure (RP) forces [5]. This mechanism is relatively weak [6], and thus OM nonlinearities demand ultralong photon and phonon lifetimes [7,8]. Semiconductor materials provide an alternative strategy through the access to exciton-mediated electrostrictive forces (based on deformation potential interaction, DP), which are enhanced at electronic resonances [9]. The question is whether this resonant enhancement can be transferred to optical resonators, if decoherence stemming from resonance-related inhomogeneous broadening and absorption can be circumvented, and if this mechanism can attain $C_0 > 1$.

Research in condensed-matter cavity optomechanics typically avoids optical absorption by working away from electronic resonances [10–13]. An unwanted consequence

is that electrostriction decreases and becomes similar in magnitude to RP [6]. Moreover, these OM resonators are intrinsically passive devices. Resonance can amplify light-sound coupling through DP interaction by several orders of magnitude, as previously demonstrated with GaAs multiple quantum wells [9,14]. Our aim is thus to translate resonant DP coupling to the context of optical resonators. By doing this, in addition, the resonators would become active OM devices. Microcavities with embedded GaAs quantum wells (QWs) at resonance in the strong-coupling regime are characterized by polaritons, quasiparticles that share the properties of the constituent photons and excitons in ratios that can be tuned through their energy difference [15]. Polariton optomechanics has been theoretically considered with prospects of new phenomena at the quantum limit [16–19]. OM nonlinearities including polariton-driven parametric self-oscillation [20,21] and asynchronous energy locking [22] have been experimentally demonstrated for many-particle condensates confined in arrays of traps. Recently, it has been argued theoretically that, in micrometer-size cavities with QWs, $C_0 > 1$ is accessible [23]. The strong-coupling regime in quantum electrodynamics has also been proposed as a means for protecting ensembles of states against decoherence induced by their inhomogeneous broadening [24,25]. In this work we show experimentally that giant values of g_0 can be indeed attained by resonant enhancement in the exciton-photon strong-coupling regime. Furthermore, we demonstrate that the OM resonant coupling is protected by the opening of the polariton Rabi gap from dephasing induced by the inhomogeneous distribution of resonant states. We present two complementary experimental approaches, namely, photoluminescence (PL) in the presence of piezoelectrically injected resonant bulk acoustic waves (BAWs) and Brillouin scattering as a function of exciton-photon detuning and temperature.

*Corresponding author: santos@pdi-berlin.de
†Corresponding author: afains@cab.cnea.gov.ar

Optical cavities with distributed Bragg reflectors also confine acoustic phonons [12,26]. We study two different microcavity structures, specifically designed for polariton modulation with electrically generated bulk acoustic waves (sample A), or for Brillouin scattering experiments (sample B). Both are planar structures (i.e., there is no lateral confinement) grown with a thickness taper to allow the continuous variation of the cavity-exciton detuning $\delta = E_c - E_x$. Here E_c (E_x) is the cavity (exciton) energy. Sample A is an (Al,Ga)As microcavity designed to confine ≈ 1.53 eV photons and $\omega_m/2\pi \approx 7$ GHz phonons [27,28]. Six GaAs QWs are positioned inside the spacer at antinodes of the optical field and close to an antinode of the acoustic strain field to enhance the DP coupling [28]. The QWs display heavy-hole (hh) and light-hole (lh) excitonic transitions separated by ≈ 5 meV, strongly coupled to the confined photon state, leading to three polariton branches with Rabi gaps of ≈ 7 and ≈ 5 meV, respectively [27]. Monochromatic phonons are injected into the microcavity using radiofrequency-driven BAW ZnO resonators, fabricated on the surface of the structure [27,29]. Sample B is a microcavity with a thick $9\lambda/2$ spacer constituted by a 41.5-period GaAs/AlAs multiple quantum well (MQW) [9,27]. A MQW is a periodically modulated acoustic structure, so its acoustic properties can be described in the band-folding scheme [30]. We perform resonant Brillouin backscattering experiments at 30 and 78 K, coupling to a $\omega_m/2\pi \approx 180$ GHz zero-group-velocity (ZGV) mode that results from this folding. Brillouin scattering is performed in double optical resonance (DOR) [31,32], i.e., the angles and energies are set so that both incoming and outgoing photons are tuned to polariton resonances of the lower branch. Figures 1(a) and 1(b) present color maps of PL spectra (10 K) obtained on sample A as a function of the BAW amplitude for negative and zero photon-exciton detuning δ, respectively. The corresponding spectra are included in the Supplemental Material (SM) [27]. These were obtained under low nonresonant optical excitation powers (below the polariton condensation threshold) and by driving the cavity with the ≈ 7 GHz acoustic mode of the resonator [27]. Below threshold, the polariton linewidth $\kappa \gg \omega_m$. In this adiabatic modulation regime the polariton lines broaden symmetrically in the time-integrated PL. Resolved sidebands are only expected for the nonadiabatic limit ($\kappa < \omega_m$). For the negative detuning in Fig. 1(a), the hh excitonic-like resonance can be identified at ≈ 1.531 eV and the cavity-like mode at ≈ 1.511 eV. It is apparent, and particularly striking in this case where the polariton modes resemble their bare constituents, that the BAWs mostly affect the exciton's energy (through DP interaction), and only very little the photon cavity mode (reflecting the weak RP contribution). The contrasting evolution of the two branches (MP excitonic and LP photonic) is indicated with dashed thin lines in Fig. 1(a). For the zero-detuning case in Fig. 1(b), the LP and MP split symmetrically around the exciton energy by the Rabi gap ≈ 7 meV, and for this detuning become modulated in similar amounts by the externally applied BAWs.

We derive the mechanically induced LP and MP energy modulation $\Delta E_{LP(MP)}$ from the PL spread of the respective mode in Figs. 1(a) and 1(b). The strain s at the QWs for a given radio-frequency power P_{RF} is calculated from the
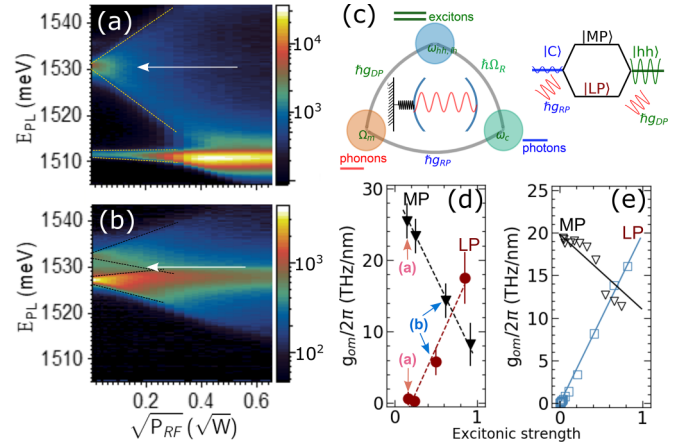

FIG. 1. (a), (b) Time-integrated polariton emission of sample A as a function of radio-frequency power applied to the piezo-electric transducer. Panel (a) corresponds to a negative detuning (-17.5 meV), panel (b) to zero detuning. The horizontal white arrow is the hh exciton energy $E_x \approx 1.530$ eV. Panel (c) is a scheme of the relevant pairwise interactions (exciton-photon $\hbar\Omega_R$, photon-phonon $\hbar g_{RP}$, and exciton-phonon $\hbar g_{DP}$) and energy levels of the optomechanical resonator with embedded QWs, in which $g_{DP} \gg g_{RP}$. Panels (d) and (e) display the experimental and theoretical optomechanical coupling factor $g_{om}/2\pi$, respectively, as a function of the exciton strength of the corresponding polariton branch (hh strength for the lower polariton LP, and lh strength for the middle polariton MP). In panel (d), solid circles (triangles) correspond to the LP (MP), and the labels (a) and (b) indicate the experimental points originated in panels (a) and (b), respectively. Dashed lines are guides to the eye. In panel (e), open squares and triangles correspond to the theoretical model presented in the text, with no adjustable parameters. The continuous lines indicate the excitonic Hopfield coefficient scaled to fit $g_{om}/2\pi$ at the largest detunings both for the LP and the MP branches.

energy injected by the piezoelectric BAW resonators and using a transfer-matrix model for the spatial distribution of the acoustic cavity mode (see details in the SM) [27]. From it we derive the displacement $\Delta u = s/q$, with q being the phonon wave number. We thus experimentally obtain $g_{om}/2\pi = \Delta E_{LP(MP)}/\Delta u$, i.e., the change of polariton (LP or MP) energy per unit displacement, which is shown in Fig. 1(d) with the dark red circles and black triangles for the LP and MP modes, respectively, as a function of the excitonic strength of the corresponding polariton mode. The excitonic strength refers to the hh component for the LP and to the lh for the MP, both of which vary from zero to one when going from very negative to very positive detuning. At very negative detuning the LP mode is mostly photonic, while the MP is hh excitonic.

$g_{om}/2\pi$ can be related to the single-particle linear OM coupling $g_0 = g_{om}x_{zpf}$ [1]. x_{zpf} is the displacement due to zero-point fluctuations and depends on the precise three-dimensional (3D) geometry of the microstructured OM resonator [23,33,34]. The maximum magnitude measured at large hh excitonic fractions is $g_{om}/2\pi \approx 20$ THz/nm. To grasp the implications of this value, one can consider a pillar of circular shape and 1.2 μm diameter for which we estimate $x_{zpf} \approx 1$ pm [27,35]. Using the measured $g_{om}/2\pi$, we obtain for this case a record $g_0/2\pi \approx 20$ MHz (see a comparison
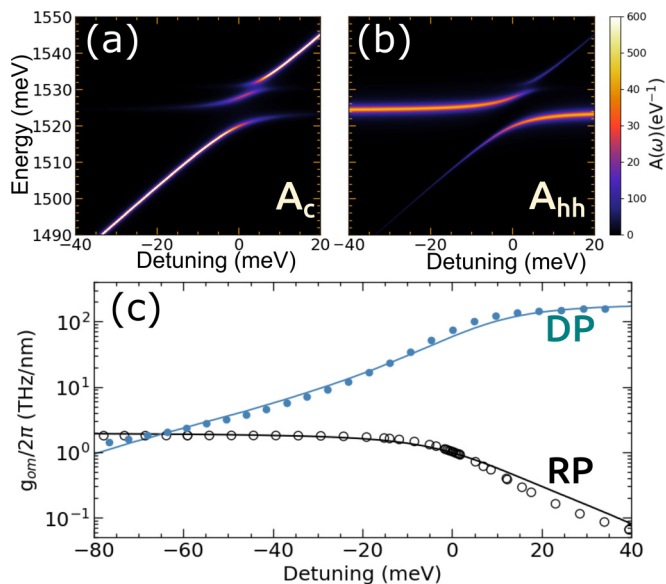
FIG. 2. Panels (a) and (b) are color-intensity maps of the photon and heavy-hole spectral weights, respectively, calculated for the polariton branches of sample B. The symbols in panel (c) are the calculated OM coupling factor $g_{om}/2\pi$, due to radiation-pressure (RP, open circles) and deformation-potential (DP, solid circles) interaction. The solid curves correspond to the scaled excitonic (DP case) and photonic Hopfield (RP) coefficients, respectively.

between different optomechanical platforms in Table II of the SM) [27]. The origin of such giant g_0 and its strong detuning dependence will be addressed theoretically next.

To introduce the model used to calculate g_0, we consider sample B. The QWs in this sample also display two energetically close hh and lh excitonic transitions, which strongly couple to the confined photon state, leading to three polariton branches [27]. The hh (lh) Rabi splitting is $\Omega_{hh(lh)} = 8.7\ (4.3)$ meV and is almost temperature independent for $T < 150$ K. The corresponding detuning dependence of the photon (A_c) and hh-exciton (A_{hh}) spectral densities, derived from PL experiments at 78 K [27], are shown in Figs. 2(a) and 2(b), respectively. $S_{c(hh)} = \int_\omega d\omega A_{c(hh)}$ is the fraction of each bare state on the coupled modes (i.e., the Hopfield coefficient). We focus our attention here on the LP branch, which evolves from purely photonic to hh excitonic when going from negative to positive detuning (the lh contribution to this state is negligible).

$g_{om}/2\pi$ [shown in Fig. 2(c)] is calculated for a planar structure as the shift induced by a mechanical perturbation on the absorptance peak associated with the LP, $A = 1 - R - T$. R and T are the reflectance and transmittance, respectively, obtained with the transfer-matrix method. The excitonic resonance is included in the dielectric function of the QWs as

$$\varepsilon(\omega) = \varepsilon_\infty + \sum_l \frac{4\pi \beta_l \omega_l^2}{\omega_l^2 - \omega^2 - i\Gamma_l \omega}$$

[36,37], where ε_∞ is the background permittivity, ω_l is the lth excitonic energy (l = hh or lh), and Γ_l is the corresponding excitonic linewidth. This model describes well the avoided

crossing between excitons and photons in the cavity [27]. The excitons' oscillator strengths $4\pi \beta_l \omega_l^2$ are set to fit the experimentally observed Rabi gaps. With a similar transfer-matrix method, the acoustic modes can also be derived [27] and, with the obtained spatial distribution, their effect on the absorptance A can be evaluated. As illustrated with the scheme in Fig. 1(c), photons interact with the excitonic component of polaritons through DP interaction, and with the photonic component through RP. The DP contribution corresponds to the effect of strain $s = \partial u / \partial z$ on the excitons' energies, included as $\tilde{\omega}_l = \omega_l - \Xi_l \times s$, where $\Xi_{hh(lh)}$ is the hh (lh) DP coefficient. RP corresponds to the change of polariton energies induced by the movement of the interfaces within the structure due to the displacement $u(z)$. We note that an additional contribution to $g_{om}/2\pi$ arises from the strain-induced variation of ε_∞. Physically, this term emerges from all DP contributions associated with higher-energy, nonresonant gaps. Its detuning dependence follows that of the RP term, with a similar magnitude [35]. For simplicity, in what follows, we consider this photoelastic contribution included within RP. Standard parameters were used for the calculation of $g_{om}/2\pi$ presented in Fig. 2(c) [27].

Two results can be highlighted in Fig. 2(c). First, except for negative detunings below ≈ -50 meV, where a crossover is observed, the DP largely surpasses the RP contribution, being approximately two orders of magnitude larger at zero detuning. Second, the overall detuning dependence of the RP and DP contributions to $g_{om}/2\pi$ follow the photonic (S_c) and excitonic (S_{hh}) Hopfield coefficients, respectively, shown with solid curves in Fig. 2(c) and scaled to fit the data at the maximum detunings. This result justifies the *ad hoc* assumption taken in Refs. [20,23], i.e., $g_0 = S_c g_0^{RP} + S_{hh} g_0^{DP}$.

The same model, when applied to sample A (only based on the specific layered structure and with no fitting parameter), leads to the lower and middle polaritons to the results shown with open squares and triangles in Fig. 1(e). Following the above discussion, we present in the same figure, with a solid blue line, S_{hh} multiplied by a constant (which corresponds to the hh g_{om}^{DP}). Based on the same considerations, for the middle polariton mode that varies from being purely hh-like to lh-like (this mode has very little photonic component [27]), the corresponding $g_0 = S_{lh} g_{0,lh}^{DP} + S_{hh} g_{0,hh}^{DP}$ [solid black line in Fig. 1(e)]. The two excitonic OM factors $g_{0,lh}$ and $g_{0,hh}$ scale as the corresponding DP coefficient $\Xi_{hh(lh)}$ (≈ 10.5 eV and ≈ 6.5 eV for the hh and lh excitons, respectively). As follows from Figs. 1(d) and 1(e), there is an excellent quantitative agreement between experiment and theory [27], strengthening our conclusion that the main contribution to g_0 is the DP interaction, which follows the detuning dependence of the excitonic component of the polariton.

Information on the detuning dependence of the OM coupling factor can also be obtained through the resonant dependence of the Brillouin intensity. This is shown in Fig. 3(a) for 30 and 78 K, for inelastic scattering by the ZGV mode at ≈ 180 GHz in sample B. Note the four-orders-of-magnitude resonant increase of the scattering efficiency observed at 30 K, comparable to that observed for a similar MQW *without* photonic confinement [9]. The detuning dependence is, however, markedly different. For the bare MQW is displayed in Fig. 3(a) with a red dashed-dotted curve, as extracted from
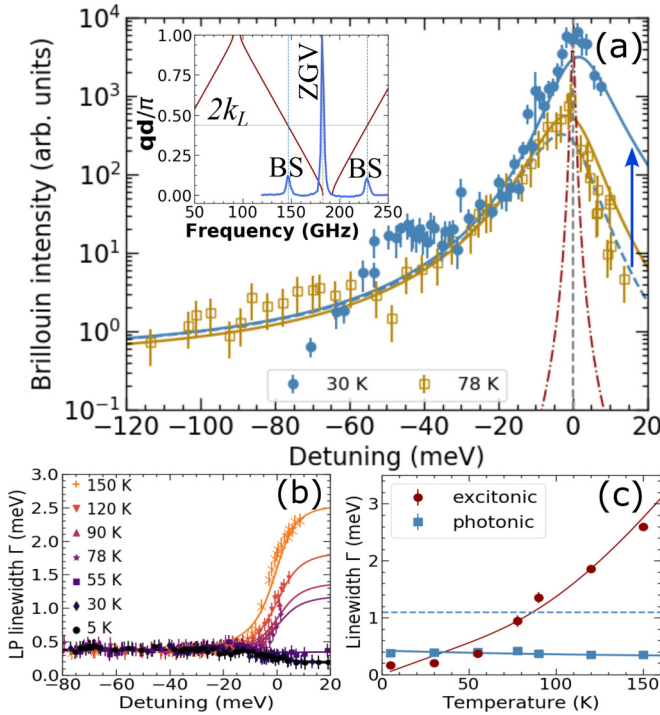
FIG. 3. (a) Brillouin scattering intensity on sample B as a function of detuning for 30 and 78 K. Symbols represent the experiments and solid curves the model. Inset shows example of a Brillouin spectrum showing the zero-group-velocity mode (ZGV), and the two backscattering peaks (BS). The phonon dispersion in the folded-band scheme is also shown. The horizontal line at $2k_L$ indicates the BS transferred wave number. The effect of inhomogeneous broadening on the 30 K case is shown with the dashed steel-blue curve (the blue arrow indicates the dephasing protection by strong coupling). The red dashed-dotted curve is the detuning dependence for an identical, but bare (no cavity confinement), MQW, as extracted from Ref. [9]. Panel (b) is the detuning dependence of the LP full linewidth at different temperatures. Panel (c) shows the extracted temperature dependence of the photon and hh exciton linewidths. The horizontal dashed line corresponds to the exciton inhomogeneous broadening. Thin solid curves in panels (b) and (c) are fits with the theoretical models explained in the text.

Ref. [9]. The steepness of this resonance is determined by the excitonic linewidth ($\approx 70\,\mu$eV at 30 K). For the microcavity with an embedded MQW in Fig. 3(a), in contrast, the detuning dependence is determined by the excitonic Hopfield coefficient (which varies over the same scale as the Rabi splitting ≈ 9 meV). The decrease of resonant enhancement with temperature, as shown in Fig. 3(a) and which for 78 K amounts to one order of magnitude, evinces the role of dephasing. We address these effects next.

Figure 3(b) presents the detuning dependence of the LP's full linewidth for different temperatures ranging from 5 to 150 K. It is observed that at 30 K the LP's linewidth is almost detuning independent (decreases slightly when going from photon to hh exciton character), while at 78 K a clear broadening occurs as polaritons become more excitonic (reflecting the phonon-induced exciton dephasing). From these data we extract the temperature dependence of the hh exciton (Γ_{hh}) and cavity (Γ_c) linewidths [38], shown with symbols in

Fig. 3(c). Γ_c turns out to be temperature independent ($\Gamma_c \approx 0.4$ meV), while Γ_{hh} monotonically increases with temperature. Its variation can be fit [39] with a linear contribution of the acoustic phonons thermal population and a second term proportional to the longitudinal optical phonon population n_{LO}: $\Gamma_{hh}(T) = 0.02$ meV $+ (1.1 \times 10^{-2}$ meV/K$)T +$ (16.6 meV)n_{LO} [shown with the solid thin curve in Fig. 3(c)] [9,39]. The zero-temperature value $\Gamma_{hh}(0) = 0.02$ meV (implying an excitonic Q factor $\approx 8 \times 10^4$) corresponds to a homogeneous linewidth [40], which contrasts with the much larger measured inhomogeneous spread of exciton states $\Gamma_{hh}^{inh} \approx 1.1$ meV [indicated with a horizontal dashed line in Fig. 3(c)]. It is quite notable in Fig. 3(b) that, at low temperatures, the LP linewidth, even at the largest positive detuning, *does not* reflect the inhomogeneous broadening of the excitonic states.

Polariton-mediated Brillouin scattering can be described as a three-step process [32]: (1) conversion of the impinging photon of frequency ω to an incoming polariton, followed by (2) the scattering of this polariton into another polariton of the same branch but different in-plane wave vector and frequency $\omega' = \omega - \omega_m$, accompanied by the emission of a ZGV acoustic phonon, and (3) the conversion of this latter polariton into an external photon, which is finally detected. This sequential process can be modeled as $I_B \propto S_c(g_0^{RP}S_c + g_{0,hh}^{DP}S_{hh})^2 S_c \Gamma_{LP}^{-2}$, where it is assumed that the phonon frequency is small so that the Hopfield coefficients corresponding to incoming and scattered polaritons are the same. Note that I_B scales as g_0^2, similar to C_0. The conversion between external photons and polaritons in both the incoming and outgoing channels leads to $I_B \propto S_c^2$. And the interaction of excitons with phonons through the DP mechanism leads to $I_B \propto S_{hh}^2$. Consequently, the maximum Brillouin efficiency occurs close to zero detuning were the product $S_c^2 S_{hh}^2$ is maximized (both Hopfield coefficients are $\approx 1/2$). This implies that only half of the maximum $g_{0,hh}^{DP}$ is typically accessed. The lifetime of the two intervening polariton states is included through Γ_{LP}^{-2} [27,32]. In this expression for I_B it is assumed that, for the LP branch, $S_{lh} \approx 0$. Theoretical results are shown with solid curves in Fig. 3(a). Because of the intrinsic uncertainty on the determination of absolute Brillouin cross sections, the experimental curve at 30 K has been scaled to coincide with the theoretical maximum, this being the only adjustable parameter valid for both temperatures. The agreement between theory and experiments is noteworthy. The quenching of the resonant enhancement with temperature is due to the broadening of the polariton line, which follows the detuning dependence of the excitonic component of the polariton (the polariton-phonon scattering is protected from dephasing due to exciton inhomogeneous broadening, but at 78 K phonon-induced homogeneous broadening is already evident). The dashed steel-blue curve in Fig. 3(a) is the calculation assuming that at 30K the hh exciton would also be affected by its inhomogeneous broadening. It is clear that the opening of the Rabi gap in the strong-coupling regime protects polaritons against such dephasing [40], remaining at low temperatures only the phonon-dependent homogeneous linewidth as the limitation factor for the fully resonant, exciton-mediated, DP OM interaction. Note that this homogeneous broadening at low temperatures is extremely small [$\Gamma_{hh}(0) = 0.02$ meV], probably reflecting the motional

narrowing effect also present in the strong-coupling regime [41–43].

To conclude, we have reported a direct experimental determination of the resonant enhancement of the OM coupling factor in distributed Bragg reflector-based microcavities with embedded QWs in the polariton strong-coupling regime. The OM coupling is dominated by the DP interaction, two orders of magnitude larger than that due to RP. Inhomogeneous broadening is avoided due to the opening of the Rabi gap. Polariton strong coupling is thus demonstrated as a path for protection against decoherence in OM applications. Based on the enhanced OM coupling, we estimate that OM nonlinearities ($C_0 \approx 1$) can be attained with pillar cavities with a diameter of ≈ 1.2 μm, and with experimentally feasible optical and mechanical Q factors $\approx 5 \times 10^4$. Polariton condensates

are also interesting due to the large coherence time of their collective phase (as compared with the decay time of individual polaritons) [21]. Based on the condensate coherence time measured in our devices (in the range 1–2 ns) [20], we conclude that as few as 2×10^3 polaritons in the condensate are required to attain the OM strong-coupling regime ($g_{eff} > \kappa_{LP}, \Gamma_m$) [44].

[1] M. Aspelmeyer, T. J. Kippenberg, and F. Marquardt, Cavity optomechanics, Rev. Mod. Phys. **86**, 1391 (2014).

[2] P. Forn-Díaz, L. Lamata, E. Rico, J. Kono, and E. Solano, Ultrastrong coupling regimes of light-matter interaction, Rev. Mod. Phys. **91**, 025005 (2019).

[3] A. Frisk Kockum, A. Miranowicz, S. De Liberato, S. Savasta, and F. Nori, Ultrastrong coupling between light and matter, Nat. Rev. Phys. **1**, 19 (2019).

[4] S. Hughes, A. Settineri, S. Savasta, and F. Nori, Resonant Raman scattering of single molecules under simultaneous strong cavity coupling and ultrastrong optomechanical coupling in plasmonic resonators: Phonon-dressed polaritons, Phys. Rev. B **104**, 045431 (2021).

[5] P. F. Cohadon, A. Heidmann, and M. Pinard, Cooling of a mirror by radiation pressure, Phys. Rev. Lett. **83**, 3174 (1999).

[6] C. Baker, W. Hease, D.-T. Nguyen, A. Andronico, S. Ducci, G. Leo, and I. Favero, Photoelastic coupling in gallium arsenide optomechanical disk resonators, Opt. Express **22**, 14072 (2014).

[7] M. Rossi, D. Mason, J. Chen, Y. Tsaturyan, and A. Schliesser, Measurement-based quantum control of mechanical motion, Nature (London) **563**, 53 (2018).

[8] H. Ren, M. H. Matheny, G. S. MacCabe, J. Luo, H. Pfeifer, M. Mirhosseini, and O. Painter, Two-dimensional optomechanical crystal cavity with high quantum cooperativity, Nat. Commun. **11**, 3373 (2020).

[9] B. Jusserand, A. N. Poddubny, A. V. Poshakinskiy, A. Fainstein, and A. Lemaître, Polariton resonances for ultrastrong coupling cavity optomechanics in GaAs-AlAs multiple quantum wells, Phys. Rev. Lett. **115**, 267402 (2015).

[10] P. T. Rakich, P. Davids, and Z. Wang, Tailoring optical forces in waveguides through radiation pressure and electrostrictive forces, Opt. Express **18**, 14439 (2010).

[11] P. T. Rakich, C. Reinke, R. Camacho, P. Davids, and Z. Wang, Giant enhancement of stimulated brillouin scattering in the subwavelength limit, Phys. Rev. X **2**, 011008 (2012).

[12] A. Fainstein, N. D. Lanzillotti-Kimura, B. Jusserand, and B. Perrin, Strong optical-mechanical coupling in a vertical GaAs/AlAs microcavity for subterahertz phonons and near-infrared light, Phys. Rev. Lett. **110**, 037403 (2013).

[13] P. E. Allain, B. Guha, C. Baker, D. Parrain, A. Lemaître, G. Leo, and I. Favero, Electro-optomechanical modulation instability

in a semiconductor resonator, Phys. Rev. Lett. **126**, 243901 (2021).

[14] M. Kobecki, A. V. Scherbakov, S. M. Kukhtaruk, D. D. Yaremkevich, T. Henksmeier, A. Trapp, D. Reuter, V. E. Gusev, A. V. Akimov, and M. Bayer, Giant photoelasticity of polaritons for detection of coherent phonons in a superlattice with quantum sensitivity, Phys. Rev. Lett. **128**, 157401 (2022).

[15] I. Carusotto and C. Ciuti, Quantum fluids of light, Rev. Mod. Phys. **85**, 299 (2013).

[16] O. Kyriienko, T. C. H. Liew, and I. A. Shelykh, Optomechanics with cavity polaritons: Dissipative coupling and unconventional bistability, Phys. Rev. Lett. **112**, 076402 (2014).

[17] J. Restrepo, C. Ciuti, and I. Favero, Single-polariton optomechanics, Phys. Rev. Lett. **112**, 013601 (2014).

[18] J. Restrepo, I. Favero, and C. Ciuti, Fully coupled hybrid cavity optomechanics: Quantum interferences and correlations, Phys. Rev. A **95**, 023832 (2017).

[19] E. S. Vyatkin and A. N. Poddubny, Optomechanical amplification driven by interference of phonon-exciton and phonon-photon couplings, Phys. Rev. B **104**, 075447 (2021).

[20] D. L. Chafatinos, A. S. Kuznetsov, S. Anguiano, A. E. Bruchhausen, A. A. Reynoso, K. Biermann, P. V. Santos, and A. Fainstein, Polariton-driven phonon laser, Nat. Commun. **11**, 4552 (2020).

[21] A. A. Reynoso, G. Usaj, D. L. Chafatinos, F. Mangussi, A. E. Bruchhausen, A. S. Kuznetsov, K. Biermann, P. V. Santos, and A. Fainstein, Optomechanical parametric oscillation of a quantum light-fluid in a lattice, Phys. Rev. B **105**, 195310 (2022).

[22] D. L. Chafatinos, A. S. Kuznetsov, P. Sesin, I. Papuccio, A. A. Reynoso, A. E. Bruchhausen, G. Usaj, K. Biermann, P. V. Santos, and A. Fainstein, Asynchronous locking in metamaterials of fluids of light and sound, Nat. Commun. **14**, 3485 (2023).

[23] N. Carlon Zambon, Z. Denis, R. De Oliveira, S. Ravets, C. Ciuti, I. Favero, and J. Bloch, Enhanced cavity optomechanics with quantum-well exciton polaritons, Phys. Rev. Lett. **129**, 093603 (2022).

[24] I. Diniz, S. Portolan, R. Ferreira, J. M. Gerard, P. Bertet, and A. Auffeves, Strongly coupling a cavity to inhomogeneous ensembles of emitters: Potential for long-lived solid-state quantum memories, Phys. Rev. A **84**, 063810 (2011).

[25] S. Putz, D. O. Krimer, R. Amsüss, A. Valookaran, T. Nöbauer, J. Schmiedmayer, S. Rotter, and J. Majer, Protecting a spin ensemble against decoherence in the strong-coupling regime of cavity QED, Nat. Phys. **10**, 720 (2014).

[26] M. Trigo, A. Bruchhausen, A. Fainstein, B. Jusserand, and V. Thierry-Mieg, Confinement of acoustical vibrations in a semiconductor planar phonon cavity, Phys. Rev. Lett. **89**, 227402 (2002).

[27] See Supplemental Material at http://link.aps.org/supplemental/10.1103/PhysRevResearch.5.L042035 for a detailed description of the studied samples and their characterization, the experimental setups, and the models used to evaluate $g_{om}/2\pi$ and the Brillouin efficiency.

[28] A. S. Kuznetsov, D. H. O. Machado, K. Biermann, and P. V. Santos, Electrically driven microcavity exciton-polariton optomechanics at 20 GHz, Phys. Rev. X **11**, 021020 (2021).

[29] D. H. O. Machado, A. Crespo-Poveda, A. S. Kuznetsov, K. Biermann, L. V. A. Scalvi, and P. V. Santos, Generation and propagation of superhigh-frequency bulk acoustic waves in GaAs, Phys. Rev. Appl. **12**, 044013 (2019).

[30] B. Jusserand and M. Cardona, in *Light Scattering in Solids V*, edited by M. Cardona and G. Güntherodt (Springer, Heidelberg, 1989).

[31] A. Fainstein, B. Jusserand, and V. Thierry-Mieg, Raman scattering enhancement by optical confinement in a semiconductor planar microcavity, Phys. Rev. Lett. **75**, 3764 (1995).

[32] G. Rozas, A. E. Bruchhausen, A. Fainstein, B. Jusserand, and A. Lemaître, Polariton path to fully resonant dispersive coupling in optomechanical resonators, Phys. Rev. B **90**, 201302(R) (2014).

[33] S. Anguiano, A. E. Bruchhausen, B. Jusserand, I. Favero, F. R. Lamberti, L. Lanco, I. Sagnes, A. Lemaître, N. D. Lanzillotti-Kimura, P. Senellart, and A. Fainstein, Micropillar resonators for optomechanics in the extremely high 19–95-GHz frequency range, Phys. Rev. Lett. **118**, 263901 (2017).

[34] F. R. Lamberti, Q. Yao, L. Lanco, D. T. Nguyen, M. Esmann, A. Fainstein, P. Sesin, S. Anguiano, V. Villafañe, A. Bruchhausen, P. Senellart, I. Favero, and N. D. Lanzillotti-Kimura, Optomechanical properties of GaAs/AlAs micropillar resonators operating in the 18 GHz range, Opt. Express **25**, 24437 (2017).

[35] V. Villafañe, P. Sesin, P. Soubelet, S. Anguiano, A. E. Bruchhausen, G. Rozas, C. Gomez Carbonell, A. Lemaître, and A. Fainstein, Optoelectronic forces with quantum wells for cavity optomechanics in GaAs/AlAs semiconductor microcavities, Phys. Rev. B **97**, 195306 (2018).

[36] A. Tredicucci, Y. Chen, V. Pellegrini, M. Börger, L. Sorba, F. Beltram, and F. Bassani, Controlled exciton-photon interaction in semiconductor bulk microcavities, Phys. Rev. Lett. **75**, 3906 (1995).

[37] Y. Chen, A. Tredicucci, and F. Bassani, Bulk exciton polaritons in GaAs microcavities, Phys. Rev. B **52**, 1800 (1995).

[38] B. Sermage, S. Long, I. Abram, J. Y. Marzin, J. Bloch, R. Planel, and V. Thierry-Mieg, Time-resolved spontaneous emission of excitons in a microcavity: Behavior of the individual exciton-photon mixed states, Phys. Rev. B **53**, 16516 (1996).

[39] D. Gammon, S. Rudin, T. L. Reinecke, D. S. Katzer, and C. S. Kyono, Phonon broadening of excitons in GaAs/Al$_x$Ga$_{1-x}$As quantum wells, Phys. Rev. B **51**, 16785 (1995).

[40] R. Houdré, R. P. Stanley, and M. Ilegems, Vacuum-field Rabi splitting in the presence of inhomogeneous broadening: Resolution of a homogeneous linewidth in an inhomogeneously broadened system, Phys. Rev. A **53**, 2711 (1996).

[41] D. M. Whittaker, P. Kinsler, T. A. Fisher, M. S. Skolnick, A. Armitage, A. M. Afshar, M. D. Sturge, and J. S. Roberts, Motional narrowing in semiconductor microcavities, Phys. Rev. Lett. **77**, 4792 (1996).

[42] H. Suchomel, S. Kreutzer, M. Jörg, S. Brodbeck, M. Pieczarka, S. Betzold, C. P. Dietrich, G. Sek, C. Schneider, and S. Höfling, Room temperature strong coupling in a semiconductor microcavity with embedded algaas quantum wells designed for polariton lasing, Opt. Express **25**, 24816 (2017).

[43] V. Savona, L. C. Andreani, P. Schwendimann, and A. Quattropani, Quantum well excitons in semiconductor microcavities: Unified treatment of weak and strong coupling regimes, Solid State Commun. **93**, 733 (1995).

[44] A. S. Kuznetsov, K. Biermann, A. A. Reynoso, A. Fainstein, and P. V. Santos, Microcavity phonoritons-a coherent optical-to-microwave interface, Nat. Commun. **14**, 5470 (2023).